

# Monte Carlo studies of the KM3NeT physics performance

Rezo Shanidze,<sup>\*</sup> Sebastian Kuch, Ulrich Katz<sup>1</sup>

*Erlangen Centre for Astroparticle Physics (ECAP), University of Erlangen-Nürnberg,  
Erwin-Rommel-Str. 1, D-91058 Erlangen, Germany*

---

## Abstract

KM3NeT neutrino telescope configurations with different detector components and geometry have been simulated and studied with modified ANTARES software. The physics performance of KM3NeT is characterised by two parameters: neutrino effective area and angular resolution of the reconstructed muons. These two benchmark parameters are determined and compared for the different KM3NeT options simulated. The physics performance of the KM3NeT configuration is evaluated by calculating achievable average upper limits for cosmic neutrino fluxes.

*Key words:* KM3NeT, neutrino telescope, MC simulation, detector performance, cosmic neutrino flux

*PACS:* 95.55.Vj, 95.85.Ry

---

## 1. Introduction

KM3NeT [1] is a future research infrastructure in the Mediterranean Sea hosting a cubic-kilometer scale neutrino telescope and nodes for deep-sea marine research. The KM3NeT consortium was formed around the institutes involved in the ANTARES, NEMO and NESTOR pilot projects [2]. In April 2008 the consortium completed the KM3NeT conceptual design report (CDR) [3].

This article reports selected results from Monte Carlo studies of the KM3NeT physics sensitivity, performed in the framework of the KM3NeT Design Study (DS), funded through the EU FP6 programme. The analysis is based on MC simulations performed with the ANTARES software modified

for KM3NeT. A detailed description of the MC studies can be found in [4], [5].

The physics performance of a neutrino telescope can be characterised by two parameters: a) the neutrino effective area  $A_{\text{eff}}^{\nu}(E_{\nu})$  and b) the angular resolution of the reconstructed muon ( $\Delta\Theta_{\mu}$ ). For a given neutrino flux  $\Phi(E_{\nu})$ , the effective area defines the neutrino event rate ( $\dot{N}_{\nu}$ ) in the telescope:

$$\dot{N}_{\nu} = \int \Phi(E_{\nu}) A_{\text{eff}}^{\nu}(E_{\nu}) dE_{\nu}. \quad (1)$$

The muon angular resolution defines the search window for the neutrino point sources and hence is an important parameter for background rejection.

The KM3NeT physics performance was evaluated as the detector sensitivity to cosmic neutrino fluxes (diffuse and point-like). The achievable average upper limits for the cosmic neutrino fluxes, calculated for one year of data taking, are presented

---

<sup>\*</sup> corresponding author: shanidze@physik.uni-erlangen.de

<sup>1</sup> on behalf of the KM3NeT Consortium

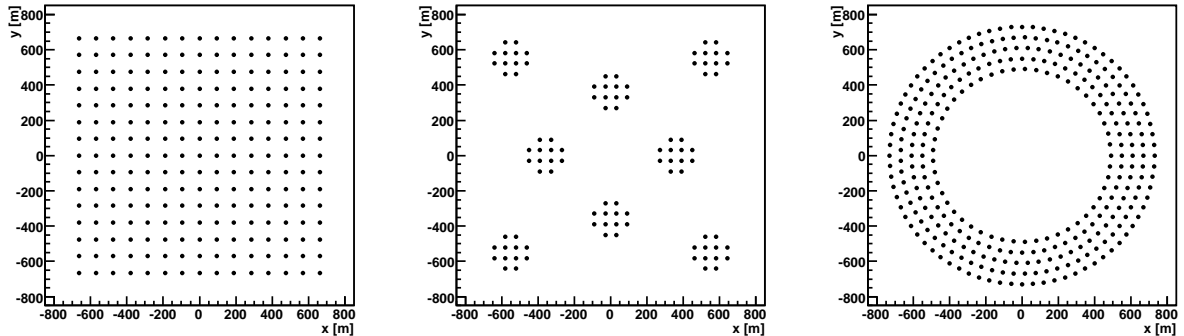


Fig. 1. An example of a seabed layout for three different KM3NeT configurations. From left to right: homogeneous, cluster and ring-type geometry configurations.

in this article.

## 2. The KM3NeT configurations

The KM3NeT configuration can be considered as a set of detector components and their geometrical layout in the deep sea. The detector components are usually assembled into deployable structures which are called detection units. We have used ANTARES-type detection units, i.e. systems of stories, where each storey can include one or several optical modules (OM) which may in turn contain a single photo-multiplier tube (PMT) or multiple PMTs.

Three different types of KM3NeT neutrino detector configurations have been studied. Examples of these configurations are shown in Fig. 1.

- homogeneous configuration (cube or cuboid type geometries);
- cluster configurations;
- ring-type configuration.

The storey and OM types which were used in these configurations are depicted in Fig. 2. They include a storey used in the ANTARES telescope as well as new multi-PMT storey/OM types developed in the framework of the KM3NeT DS [6].

For the comparison of different detector configurations, the instrumented volume ( $1 \text{ km}^3$ ) and the total photo-cathode area of all detectors were fixed within 5%. Several options with different storey

types have been considered for each geometric configuration. The total length of the detection unit from the sea bed to the uppermost element (buoy) for all configurations was about 700 m, with the first storey situated at 100 m from the bottom.

## 3. The MC simulations

For each detector configuration more than  $10^9$  muon neutrino ( $\nu_\mu$ ) charged current (cc) interaction events,

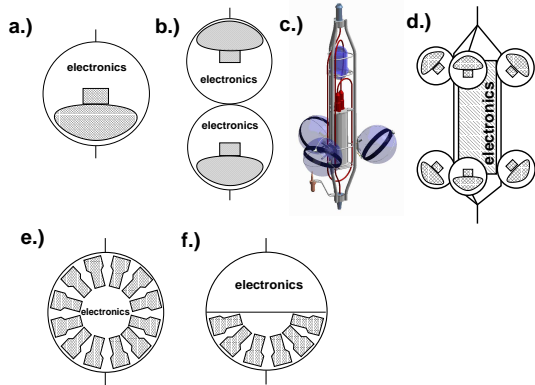


Fig. 2. Different storey and OM types used in the simulations: a) storey/OM with 1 large ( $10''$ ) PMT; b) storey with 2 OMs; c) ANTARES type storey; d) storey with 6 OMs. Multi-PMT storeys with small ( $3''$ ) PMTs: e) spherical storey with 42 PMTs; f) spherical storey with 21 PMTs.

$$\nu_\mu + N \rightarrow \mu + X, \quad (2)$$

have been simulated for the neutrino energy range  $10 \text{ GeV} < E_\nu < 10 \text{ PeV}$ . The angles of incidence were isotropically distributed over  $4\pi$ . The interaction vertices for  $\nu_\mu$ -cc events were simulated in an extended volume, taking into account the muon propagation length and Cherenkov light attenuation in sea water. The Mediterranean Sea water model, developed in the ANTARES collaboration, was used in the simulations [7]. For each event the Cherenkov photons from the muon were simulated and transported to the OMs. In the next step the PMT hits were generated and stored for further analysis. The final hit sample also includes randomly distributed PMT hits from  $^{40}\text{K}$  decays in the sea water ( $\approx 100 \text{ Hz/cm}^2$  of photo-cathode area)

After event reconstruction, the neutrino effective area and muon angular resolution were calculated. As an example, the effective areas for the homogeneous and cluster-type configurations and their ratios are presented in Figs. 3 and 4. This example indicates that cluster configurations, due to dense instrumentation inside the clusters, have a larger effective area at lower energies ( $E_\nu < 1 \text{ TeV}$ ), while at higher energies  $A_{\text{eff}}^\nu(E_\nu)$  is significantly smaller. The ring type configurations show a similar behaviour at low energies, however the large empty volume inside the detector reduces  $A_{\text{eff}}^\nu(E_\nu)$  for small zenith angles.

The muon angular resolution as a function of neutrino energy shows the similar behaviour for all configurations. Above  $E_\nu > 10 \text{ TeV}$  the muon

angular resolution is better than  $0.1^\circ$ .

The comparison indicates that no detector configuration is superior over the whole energy interval considered. In the energy range above  $1 \text{ TeV}$ , homogeneous detectors have a slightly larger effective area in comparison to ring type detectors, therefore this configuration was selected as a reference configuration with 225 (15x15) strings, each carrying 37 storeys with multi-PMT OMs ( $21 \times 3''$  PMT, see Fig. 2f). The distances between stings are  $95 \text{ m}$  and vertically between storeys  $15.5 \text{ m}$ .

#### 4. Physics performance

The physics performance for the KM3NeT reference detector was studied for  $E^{-2}$  type cosmic neutrino fluxes. The number of expected signal and background events was calculated from equation (1). The Bartol model [8] was used for the atmospheric neutrino flux. The upper limits for the cosmic neutrino fluxes were evaluated from

$$k_\nu^{\text{limit}} = \frac{N_s^{\text{limit}}}{N_A} k_A, \quad (3)$$

where  $N_A$  is a number of cosmic neutrino events for an arbitrary flux  $k_A E^{-2}$ , and  $N_s^{\text{limit}}$  corresponds to an average upper limit that could be obtained from the recorded data in the absence of a signal.  $N_s^{\text{limit}}$  and the corresponding average upper limit at 90% C.L. was obtained with the Feldman and Cousins method [9]. The results for the reference

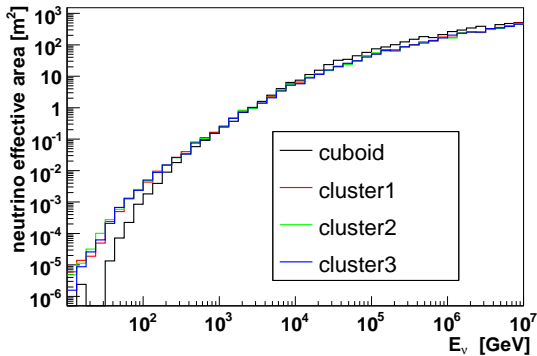


Fig. 3. Calculated neutrino effective areas for the homogeneous cuboid and 3 different cluster type detectors.

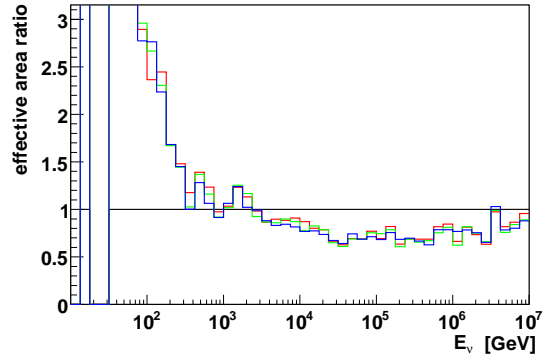


Fig. 4. Effective area ratios of cluster configurations to the homogeneous (cuboid) configuration (line).

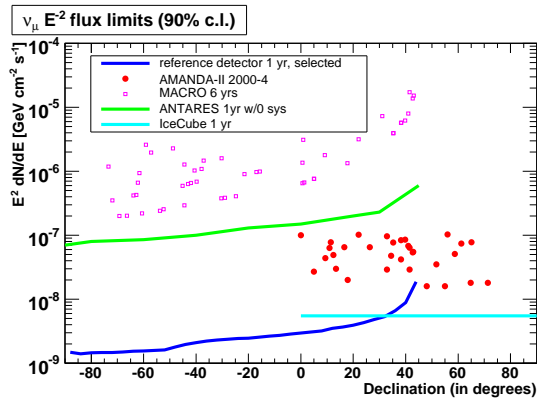


Fig. 5. Average flux limit for point sources vs. declination for the KM3NeT reference detector, calculated for  $\nu_\mu$  events. For comparison, the experimental results from AMANDA and MACRO are plotted together with expected limits from the ANTARES and IceCube neutrino telescopes.

detector are given in Figs. 5 and 6. The references for the experimental data used in these figures can be found in [5].

All limits presented here are preliminary. The algorithms used are not yet optimised for the KM3NeT configurations and no energy reconstruction has been performed.

## 5. Conclusions

Different configurations of the KM3NeT neutrino telescope were simulated and studied with modified ANTARES software. None of the studied KM3NeT configurations is superior over the full energy range. Therefore it is crucial to define the physics priorities for the KM3NeT neutrino telescope.

The KM3NeT neutrino telescope can set upper limits on cosmic neutrino fluxes which are about 50 times more stringent than expected limits from the ANTARES project. It should be noted that an average upper limit for the diffuse neutrino flux obtained for the KM3NeT reference detector is well below the expected theoretical value predicted by Waxman and Bahcall [10].

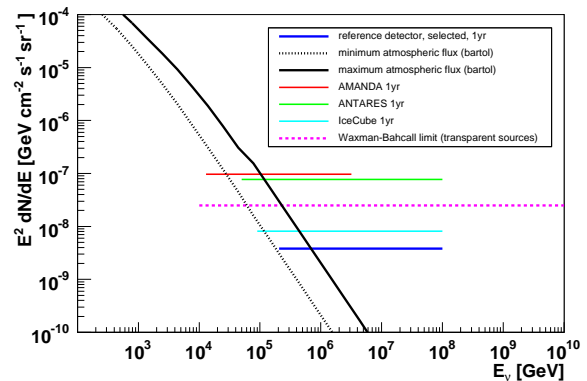


Fig. 6. Average diffuse flux limit for the KM3NeT reference detector, calculated from  $\nu_\mu$  events. The experimental upper limits from the ANTARES and IceCube detectors are also plotted together with the atmospheric neutrino flux and the theoretical Waxman-Bahcall limit.

## 6. Acknowledgements

This study was supported by the European Commission through the KM3NeT Design Study, FP6 contract no. 011937. The authors would like to thank the organisers of VLvNT-2008 for their hospitality and a perfectly organised workshop.

## References

- [1] [www.km3net.org](http://www.km3net.org)
- [2] U. F. Katz, Prog.Part.Nucl.Phys. 57 (2006) 273-282, Nucl.Instrum.Meth. A567 (2006) 457-461
- [3] U. F. Katz, these proceedings.
- [4] S. Kuch, Nucl. Instrum. and Meth., A567 (2006), 498
- [5] S. Kuch, Ph.D. Thesis, FAU-PI1-DISS-07-001, 2007. [www.opus.ub.uni-erlangen.de/opus/volltexte/2007/692/](http://www.opus.ub.uni-erlangen.de/opus/volltexte/2007/692/)
- [6] P. Kooijman, Nucl. Instrum. and Meth., A567 (2006), 508
- [7] J. A. Aguilar *et al.* [The ANTARES Collaboration], Astropart. Phys. **23** (2005) 131
- [8] G. Barr, T. K. Gaisser, T. Stanev, Phys. Rev. D 39 (1989), 3532
- [9] G. J. Feldman, R. D. Cousins, Phys. Rev. D 57 (1998), 3873
- [10] E. Waxman, J. Bahcall, Phys. Rev. D 59 (1999), 023002